
This is an electronic reprint of the original article.
This reprint may differ from the original in pagination and typographic detail.

Elmas, Serenay; Filz, Günther H.; Markou, Athanasios; Romanoff, Jani
Zero Gravity: a novel cantilever beam utilizing elastic torsion for structures and architecture

Published in:
<i>Proceedings of IASS Annual Symposia</i>

Published: 01/08/2021

Document Version
Peer reviewed version

Please cite the original version:
Elmas, S., Filz, G. H., Markou, A., & Romanoff, J. (2021). Zero Gravity: a novel cantilever beam utilizing elastic torsion for structures and architecture. In *Proceedings of IASS Annual Symposia* (Vol. 2021). (Proceedings of IASS Annual Symposia). International Association for Shell and Spatial Structures (IASS).
https://www.researchgate.net/publication/354091092_Zero_Gravity_a_novel_cantilever_beam_utilizing_elastic_torsion_for_structures_and_architecture

This material is protected by copyright and other intellectual property rights, and duplication or sale of all or part of any of the repository collections is not permitted, except that material may be duplicated by you for your research use or educational purposes in electronic or print form. You must obtain permission for any other use. Electronic or print copies may not be offered, whether for sale or otherwise to anyone who is not an authorised user.

Zero Gravity: a novel cantilever beam utilizing elastic torsion for structures and architecture

Serenay ELMAS*, Günther H. FILZ, Athanasios A. MARKOU^a, Jani ROMANOFF^b

* Aalto University, ENG | Department of Civil Engineering ° ARTS | Department of Architecture
Rakentajanaukio 4 A, 02150 Espoo, Finland
serenay.elmas@aalto.fi

^a Aalto University ENG | Department of Civil Engineering

^b Aalto University, ENG | Department of Mechanical Engineering

Abstract

This paper describes the structural geometry of a beam element, which is assembled from 4 coupled, thin elastic strips through intentionally applied torsion. Consequently, the beam element generates a self-restraining system. Our investigations are based on architectural design studies of preliminary paper models, laboratory experiments of the full-scale cantilever beam, and computational structural simulations. We are also providing a comparison between digital, physical, and photogrammetric results. We describe the production, assembly, disassembly, the shape generation principles, and the final shape of the beam element in various scales from paper model to physical prototype. We are exploring the design and application space as well as the digital generation and the digitalization of the beam geometry. The paper pays special attention to the geometrical stiffening effect, which has been described by the Föppl-von Kármán (FvK) equations. The phenomenon of notably undulating surfaces of the individual strips of the beam is associated with their length-to-width-ratio but mainly with the extremely thin material thickness. The utilization of elastic torsion as a design driver links structural efficiency, architectural potentials, and aesthetics as first demonstrated in the realized research pavilion “Zero Gravity” by the team of A”SA (Aalto University Structures and Architecture) in 2019.

Keywords: structures and architecture, lightweight structures, self-organizing, bending active, elastic torsion, torsional bending active structures, geometric stiffening, Föppl-von Kármán

1. Introduction

Torsion, apart from twisting in non-circular cross-sections, causes warping, which results in nontrivial geometry (Timoshenko [1]). The interest in the generation and investigation of twisted geometries have a long history that dates back to ancient times (Cartwright and Gonzalez [2]). Nevertheless, torsion usually has not been considered as beneficial or desired from both structural and material perspectives (Wise [3]). However, there are many examples of twisted elements or structures throughout architectural history. Besides aesthetic or ornamental purposes, in some cases, twisted geometry has been the result of conceptual [4], functional or structural [5] considerations. Our approach to elastically torqued structures is, to intentionally use twisting as a method for the coalesce generation of architectural forms and efficient, load-bearing structures through utilizing the embodied elastic, residual stresses. Therefore, the presented method and process combines simultaneously bending-active (Lienhard [6]) aspects with torsion as a design driver of and for the proposed element. Depending on the achieved equilibrium states, the resultant geometry provides very light and highly efficient structures in both, material use and structural performance perspectives accompanied with compelling architectural and functional features.

This paper presents the geometry of an elastically torqued beam element at such an equilibrium state, applied as a cantilevering beam element of the Zero Gravity kinematic pavilion, (Filz et al. [7]). Our investigation focuses on the self-organizing geometry, as well as on the structural and architectural potentials of the elastically torqued beam element. The current work is based on architectural design studies through preliminary paper models, on laboratory experiments of the full-scale cantilever beam, as well as on the comparison between computational simulations and photogrammetric analysis.

2. Production, assembly, disassembly, and shape of the beam element

2.1. Creating a beam element from four twisted strips

A single, elastically twisted strip can provide functional features as part of a larger structure. On the other hand, such a strip usually cannot generate an efficient load-bearing system as a primary structure. In architectural applications, bending-active strips have been used as twisting parts of kinetic façades like in the Softhouse project (Lienhard and Knippers [8]) and the Yeosu Pavilion (Knippers et al. [9]) among others, functioning as a shading system. Another approach has been followed in the Loops experimental structure (Filz [10]), focusing on the exploration of possible forms achieved by elastic torsion. Combining geometrical and structural aims with functional features demands for a global restraining system. Along these lines, torqued strips have been employed in hybrid structures (Slabbinck et al. [11]) to increase their stiffness capacity or in grid-like structures such as in the Berkeley Weave (Schleicher and La Magna [12]). In contrast to the above-mentioned systems, we are proposing an approach by using four torqued strips to create a closed structural geometry by simultaneously generating a self-restraining system. Such a beam element follows a formation process, where both the resulting global geometry and the geometry of the individual strips are the results of a self-organizing process.

2.2. Shape generation principles

The concept for the shape generation of the proposed beam element is demonstrated in figure 1. Firstly, a tube of square cross-sectional shape (figure 1b) is created by repetitively folding a rectangular sheet of paper (figure 1a) three times. Secondly, the obtained 1 degree-of-freedom (DOF) mechanism is locked by cross-wisely connecting the tube's short edges (figure 1c). On one hand the individual paper segments (strips) are not constrained by support conditions. Therefore, they are free to spatially rearrange during twisting. On the other hand, the four individual strips are interdependent due to the hinge coupling of the strips' longitudinal edges. This method of restraining the mechanism relies on the deformation of the individual paper segments (strips). Consequently, the linear edges of the paper segments (strips) transform into the common seamlines between the strips described by planar curves (figure 2). In the resulting geometry, these seamlines work as proper hinges along the longitudinal edges of the four rectangular paper segments (strips), which have been torqued by 90° , or more specifically by two times 45° in opposite directions.



Figure 1: The generation principles of the shape through a paper model: (a) a piece of paper with four segments, (b) folding a square cross-section tube, (c) cross-wisely connecting the tube's short edges to restrain the 1-DOF-mechanism

Simultaneously, a sideward shift of each of the four paper segments (strips) occurs besides their twist of 90° . The horizontal and vertical shifts of each segment (strip) are equal to their half widths. Consequently, the central axis of the created tube describes the intersection line and the central axis of the beam element's mirroring planes (horizontal and vertical) before and after closing the system, as shown in figure 2. Such a formation process causes considerably large, geometrically non-linear deformation, which requires adequate flexibility from the material point of view. To achieve the desired geometry, we use extremely light, thin, and elastic material by using parts of the materials' capacity [13] for the twist procedure. In return, the resulting inner force balance and stresses can increase the global, geometrical stiffness of the beam element. In short, we are selling parts of the material's strength for gaining increased stiffness. One of the striking features of paper models is the undulating surface of each single paper segment (strips), which was initially thought to be an imperfection of model making but has very specific reasons and benefits, which will be discussed in section 5.

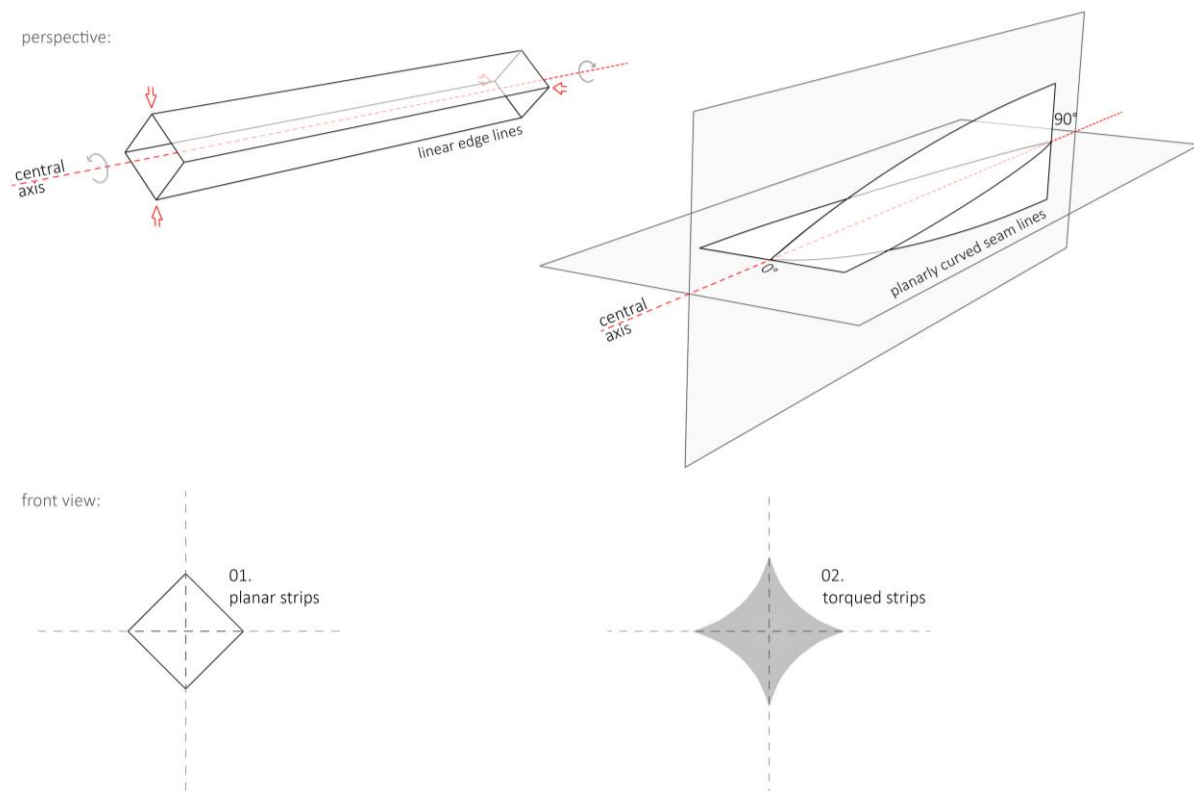


Figure 2: The concept of the formation process with respect to the unchanged central axis, mirroring planes, the sideward shifts of the strips, and the transformation of strips' linear edge lines into planarily curved seam lines

2.3. Full-scale prototypes from plywood strips

Our investigations include a series of physical models in various scales from different thin sheet materials in different thicknesses. Accordingly, the closed, hollow-section cantilever beam element, shown in figure 3, was assembled from four identical, plywood strips. The strips were cut from planar plate material of 6.5mm all-birch plywood composed from five veneer layers, with three layers in cross direction and two layers in longitudinal direction, and with $E_{m \parallel}$: 12737 N/mm² and $E_{m \perp}$: 4763 N/mm² as the most relevant material properties amongst others [14]. The material dimensions and the orientation of the plies were defined with respect to flexibility properties for the practical formation process. So, the decision for plywood as material included aspects like practicability, ease of processing, ease of assembly and sustainability. The selected material thickness was based on manual testing and

availability as an industrial product. The strips' width-to-length ratio was chosen as 1/10, which turned out to be an appropriate ratio according to the above-mentioned experiments and material tests. Similar to our initial paper models, the width-to-length-to-thickness ratio of the individual plywood strips can be considered as very thin. Consequently, the beam element's strip dimensions were 200mm width \times 2000mm length \times 6.5mm thickness. A 400mm overlength was left for clamping the beam element during the load tests and for connecting it to other members of the roof structure of the Zero Gravity pavilion (figure 3).

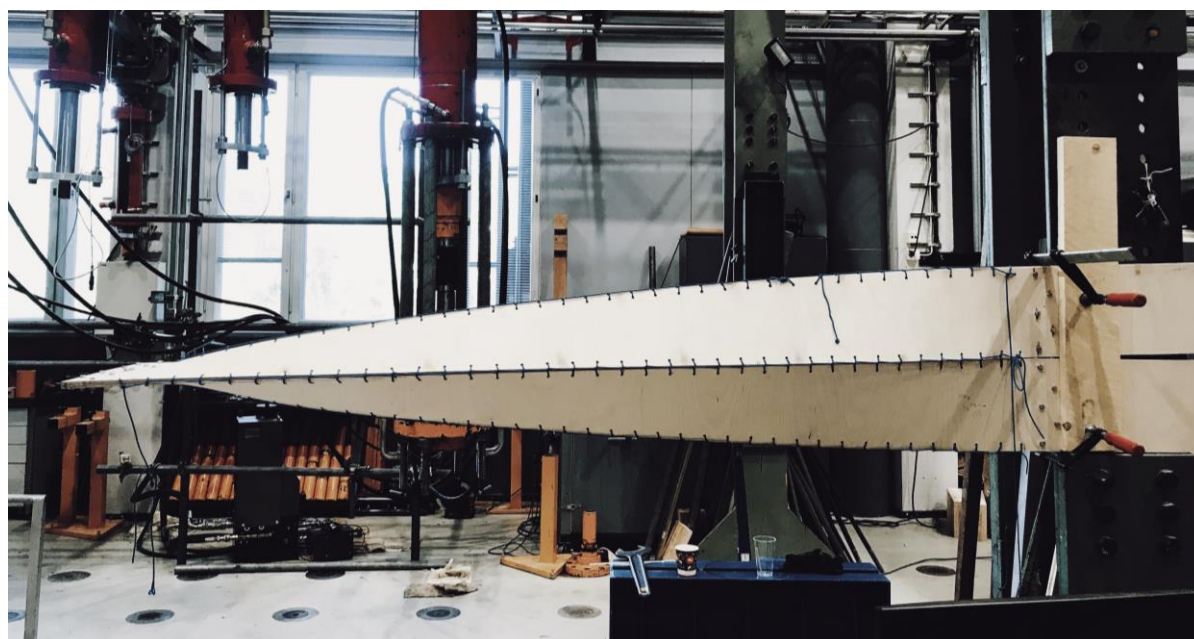


Figure 3: Cantilevering beam prototype from four torqued plywood strips with laced seamlines, clamped free end, and overlength of strips clamped to support

In contrast to the paper models, which are formed from one tube into the structure, the full-scale beam element is assembled from separate strips in two steps: (i) by twisting each of the four initially planar strips by 90 degrees around their longitudinal axis, and (ii) by assembling the inversely twisted strips into a hollow profile to generate matching seamlines. Clearly, elastic bending around the two different axes, namely the weak (perpendicular to the longitudinal axis) and the strong (perpendicular to the plane) ones of the plate considerably influences the final geometry. Following twisting each individual strip, the longitudinal seamlines are hinge joined, while the short edges are closed by clamping for practical reasons. An area of 5cm width was used for the clamping at the both ends of the element. This led to the lenticular openings in-between the strips as shown in figure 4a. These openings were gradually closed by employing the “Clove Hitch End” lacing technique [15]. The used lacing material was standard, 100% multifilament braided polypropylene rope with a diameter of $\varnothing 4$ mm. The rope is fed through predrilled holes of the thin plywood strips and then between itself to create a crossing point, which ends up in a friction based self-locking system (figure 4c). The utilized self-locking system does not necessitate knots, consequently it provides quick closing, the possibility of adjusting and re-opening. This process of assembly generates common seamlines, which naturally follow planar curves. Of course, the overall geometry of the beam and the longitudinal seamlines are slightly deviating from a purely hinged version as described above by the paper models, but in this stage of research, the deviations are assumed as less relevant.

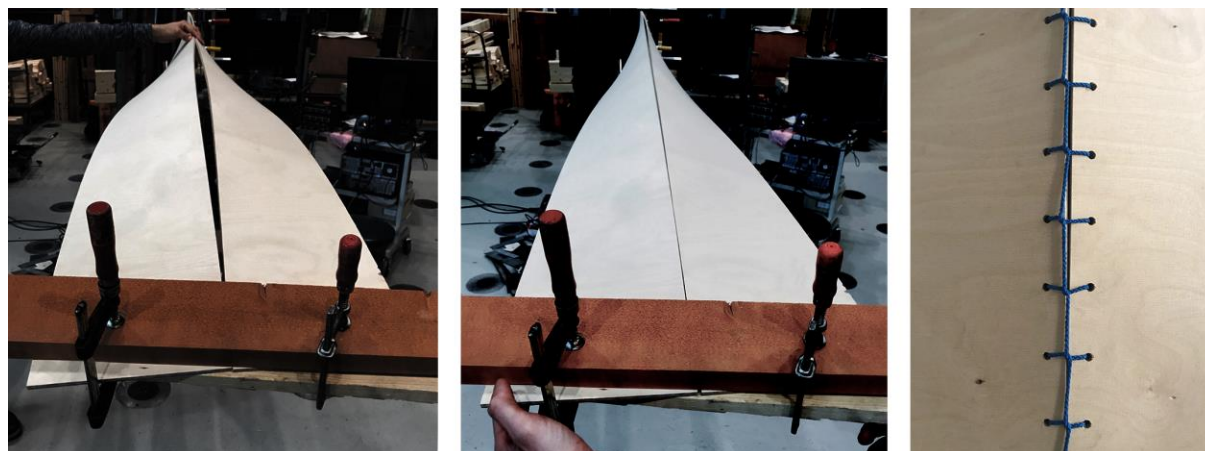


Figure 4: (a) Lenticular opening in-between the strips, (b) closed opening, (c) generated laced seamlines detail

Similar to the paper folded version, one person can manually conduct all steps of the formation and the assembly process of the beam element with common tools. Ease of manufacturing, assembly, and rapid disassembly has been achieved by using flat sheet material (as provided by the industry), simple, rectangular cutting patterns without cut off and by applying proposed low-tech detailing for the seamlines. Yet, the achieved geometry does show high complexity: shape-wise through its global fluent form with undulating surfaces and structure-wise through combining material properties with geometric stiffness.

3. Design and application space

As a first validation of application, the above-presented beam element was used in a full-scale experimental structure, namely the “Zero Gravity” kinematic pavilion. [7] (figure 5a). Six elastically torqued beam elements were employed as cantilevering beams of the roof of the pavilion (figure 5b). The cantilevering application enables the utilization of the full potential of the beam's geometry by following the natural force flow and shape of a cantilever. Accordingly, the horizontal edges (smallest vertical cross-section) were forming the cantilever's free end, where the bending moment is zero. The beams' vertical edges (tallest vertical cross-section) providing the maximum structural height where the maximum bending moment is expected to occur (figure 6).

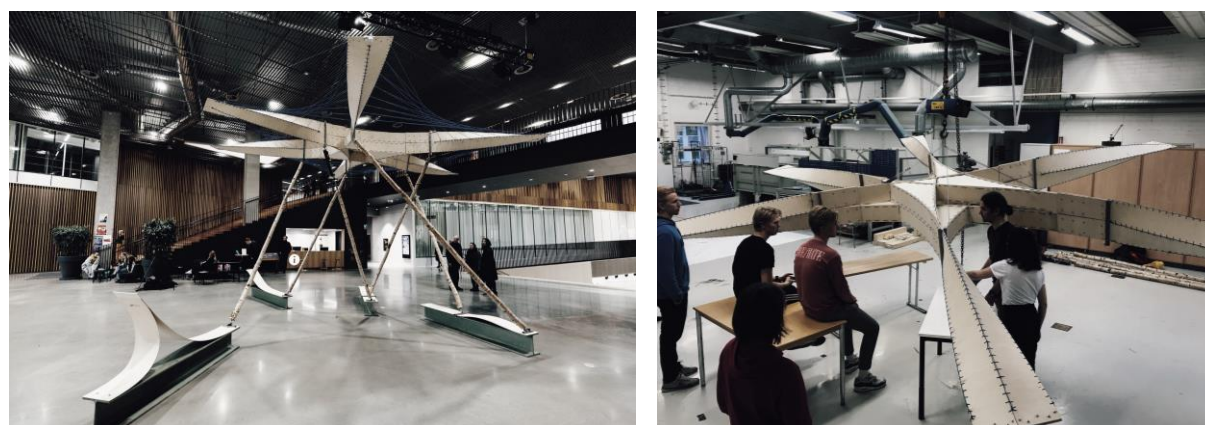


Figure 5: (a) Zero Gravity Kinematic Pavilion, a full-scale prototype, (b) roof of the pavilion

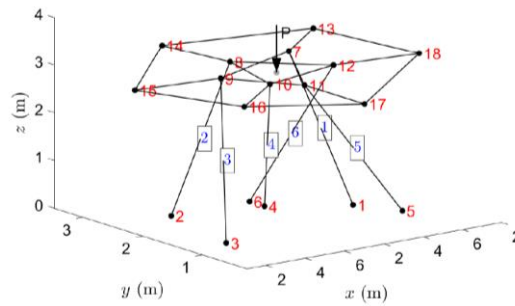


Figure 6: Structural model, numbers from 7 to 12 denote the points, where cantilevering beams are connected to the roof

However, the horizontally cantilevering beam is only one type of application within a wide range of constellations. The design and application space includes mirrored versions as a simply supported beam-element and variations of the strips' cutting pattern in shape and/or ratio. The modification of the beam's short edges (in the present case 90° and orthogonal to the central axis) allows for changes in the spatial orientation and the number of connected beam elements with the potential of creating spatial structures. This potential will for example lead to spatial branching and/or grid-like, planar, or spatially arranged structures, which are not the subject of this paper.

4. Digital generation and the digitalization of the geometry

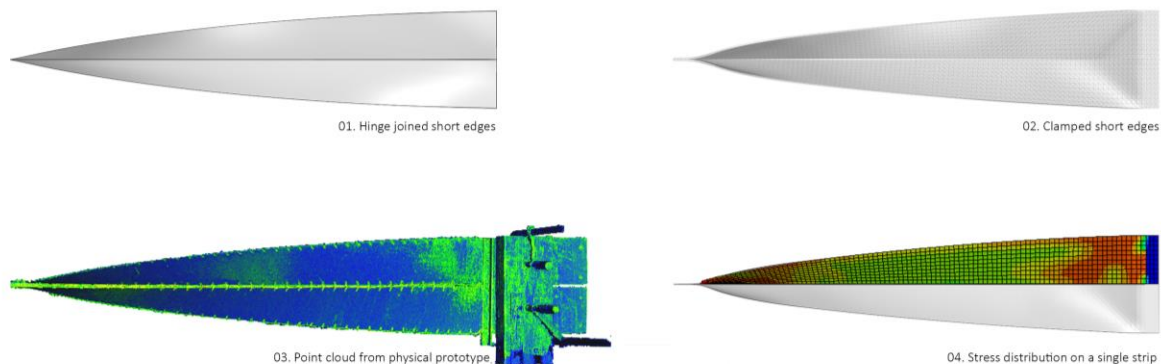


Figure 7: Geometric models with (a) hinged and (b) clamped short edges, (c) photogrammetric reconstruction of the beam element, expresses the number of points per square meter and (d) Von Mises stresses of a single strip

The digital generation of the shape is conducted in the Rhinoceros 6 SR34 and Grasshopper environment [16] with Kangaroo 2 physics engine, and Abaqus CAE FEM software [17] by using thin-shell elements (S4R). In our computational models, the short edges were assumed to be closed as hinge-joined (according to the paper model) or as clamped (as executed in the full-scale prototype) (figure 7a-b). However, we used the digital model with clamped short edges, to compare the digitally generated geometry with the geometry of the physical, full-scale prototype.

To increase computational efficiency, the investigations have been conducted based on a single strip by introducing the constraints imposed by the neighboring strips. Accordingly, one of the longitudinal edges of the strip is restrained to lie in a predefined horizontal plane, while the other longitudinal edge is forced to lie in a vertical mirroring plane, as shown above in figure 2. The initial and the final position of the short edges are defined. Along with 90° rotation, a vertical and horizontal displacement in y and

z directions is imposed by half of the strip's width as described in section 2.2, while the translation in the x-direction is not restricted. Computationally both, the rotational movement of 90° and the translational movement are not directly induced to the strip, but they are imposed on a secondary element, which is connected to the strip's free short edge. Correspondingly, the algorithm let all the vertices allocate themselves as a result of the connected element's rotation and translation within the limits of defined boundary conditions. Quasi-static (Clough and Penzien [18]) analysis is used to simulate the large deformation for gradually increased torsion in geometrically non-linear FEM (figure 7d).

The realized beam prototype was digitalized in a photogrammetric reconstruction by using the RealityCapture software [19] through following the methodology described by Janiszewski et al. [20]. The mesh model was generated from 3D point cloud consisting of 9 million points with a mean surface point density of 5 pts/mm² (figure 7c). This digitalization served as a reference model, which was overlaid with the generated mesh from computational simulation. As a result, the maximum, spatial deviation of the compared mesh-geometries was about less than 4mm. Compared to the size of the individual strips, which are 200mm width × 2000mm length × 6.5mm thickness, this deviation is considered as minor.

5. Geometrical stiffness and the Föppl-von Kármán effect

The resulting, form found shape of the beam's geometry is a consequence of a displacement-driven process because we know the dimensions of the strips, their coupling, the final, spatial position of the short edges, and that the longitudinal seam-lines are either part of a vertical or a horizontal plane as shown in figure 2.

As mentioned above, the individual strips' longitudinal edge lines turn into planarly curved seamlines of the final beam element. Although the longitudinal edges of the strips tend to describe spatial curves during twisting, they are inherently forced to follow the planar curves due to sharing common seamlines. In response, undulating stripe-surfaces emerge from the increased inherited stresses. This phenomenon, which is associated with the small material thickness, has firstly been noticed in our paper models. However, all the physical prototypes generated from very thin strips show notably seen undulating surfaces as a result of self-equilibration of the structure. The observed structural phenomenon is related to what has been described by the Föppl-von Kármán (FvK) equations in terms of stress resultant, which can have a geometric stiffening effect on structures against external loading.

The ratio between the typical dimension of the plate a and its thickness h , namely a/h , of the typical strip used in the beam prototype shown in figure 3, lies between $10 < a/h < 100$ and according to Ventsel [21] the plate is classified as thin plate. Furthermore, these types of plates are further classified according to the deflection w to thickness h ratio, namely w/h , as stiff for $w/h < 0.3$ and as flexible when $w/h > 0.3$. Additionally, when the magnitude of ratio w/h is larger than 5, the membrane behaviour dominates the response. In these cases, the linear plate bending theory of Kirchoff [22] is not valid anymore due to the fact that it neglects the straining of the middle plane of the plate along with its corresponding stresses. To this end, the large deflection theory of thin plates applies and more specifically the coupled nonlinear partial differential equations first developed by von Kármán [23] hold:

$$\frac{\partial^4 \phi}{\partial x^4} + 2 \frac{\partial^4 \phi}{\partial x^2 \partial y^2} + \frac{\partial^4 \phi}{\partial y^4} = Eh \left[\left(\frac{\partial^2 \phi}{\partial x \partial y} \right)^2 - \frac{\partial^2 w}{\partial x^2} \frac{\partial^2 w}{\partial y^2} \right];$$

$$\frac{\partial^4 w}{\partial x^4} + \frac{\partial^4 w}{\partial x^2 \partial y^2} + \frac{\partial^4 w}{\partial y^4} = \frac{1}{D} \left(p + \frac{\partial^2 \phi}{\partial y^2} \frac{\partial^2 w}{\partial x^2} + \frac{\partial^2 \phi}{\partial x^2} \frac{\partial^2 w}{\partial y^2} - 2 \frac{\partial^2 \phi}{\partial x \partial y} \frac{\partial^2 w}{\partial x \partial y} \right) \quad (1)$$

where Φ denotes the stress function due to geometrical non linearity (von Kármán), w the normal to the surface deflection of the plate, E the modulus of elasticity, h the thickness of the plate and $D = \frac{Eh^3}{12(1-\nu^2)}$, where ν is the Poisson ratio and p the normal to the plate surface load. The relationship between the stress function Φ and membrane forces is given by the following equations:

$$N_x = \frac{\partial^2 \Phi}{\partial y^2}; N_y = \frac{\partial^2 \Phi}{\partial x^2}; N_{xy} = \frac{\partial^2 \Phi}{\partial x \partial y} \quad (2)$$

The equations (1) hold for isotropic material and for orthotropic with not large ratio between their modulus of elasticity. The first of the equations (1) represents the in-plane equilibrium equation, while the second one represents the bending. When the deflections are small, the two equations decouple, and the latter equation is only needed to solve the plate bending. Then the righthand side reduces to p/d . Due to the complexity of the analytical solution of equations (1), a finite element simulation was used to derive the response of the plate.

The numerical simulation implemented in Abaqus [17] indicated that at some parts of the strip the membrane stresses are dominating the response of the plate, compared to the flexural ones. More specifically, at the regions close to the ends of the beam, where the deflections are large, the membrane stresses were dominant. As the case study shows, the torque related curvature and the geometrical non-linearity activate the membrane stresses at the plate middle surface at the regions close to the ends of the beam. This effect is due to the von Kármán strains, see Eq. 1, which couple the relatively large out-of-plane deflections to the in-plane responses.

6. Conclusion and outlook

Although torsion usually is not considered beneficial from structures and material perspectives, our studies indicate high architectural potential and significant structural benefit due to the geometrical stiffening effect, which has been described by the FvK equations. Presented beam element shows one aspect of the ongoing research in the framework of elastic torsion as a design driver for architectural aesthetics and applications as well as structural performance. We presented the structural geometry of a beam element from four torqued strips for lightweight structures. The beam element has been evaluated through its successful use as a cantilevering beam element of the “Zero Gravity” kinematic pavilion with a pre-defined set-up, width to length ratio of 1\10, and 6.5mm thickness. The proposed assembly method and the coupling and utilization of elastic torsion of the four individual thin strips result in a geometry that follows the natural force flow and shape of a cantilever beam. The cantilever beam was tested against bending, and as a result, the point-load applied at the cantilever's free end has been approximately twenty-five times the beam's self-weight.

Our investigations are including computational structural simulations for shape generation, geometrical and structural analysis. The comparison of the digital and the physical prototyping are based on photogrammetric reconstruction. The results show highly precise matches in shape and structural performance. The described low-tech methods for assembly have been architecturally interesting and structurally sufficient for our early stage experiments. They also have a huge impact on the disassembly of the structure. The beams' self-weight of less than 10kg, strips with cutting patterns without cut-offs and the use of natural material (plywood) are important aspects in the light of sustainability.

Our ongoing explorations of the design and application space open new avenues for spatial lightweight structures in various scales and are connected to studies on the reciprocal relationship of the dimensions, the shapes of the cutting patterns of the strips and the loadbearing capacity of the resulting structural elements. As our preliminary results indicate, there are cases where thinner material will increasingly

activate the geometrical stiffness and especially the FvK-effect, we will continue our ongoing parametric study on comparing specifically predefined elements regarding their material thickness. This way we identify a possibility to increase the strength of structural members by saving material and self-weight, which might be of importance for some industries and one aspect of finding more environment friendly solutions.

Future studies will exploit the further geometric potential of the formation process by changing the cutting patterns, the way the strips are coupled (clamped vs. hinged), the angle of induced rotation, and the scale with respect to its limits and qualities. Our interests and considerations include fields like the shipbuilding industry and applications with aerodynamic requirements.

References

- [1] Timoshenko S. Strength of materials, part II. Advanced theory and problems. 1941;245.
- [2] Cartwright JHE, González DL. Möbius Strips Before Möbius: Topological Hints in Ancient Representations. *The Mathematical Intelligencer*. 2016;38(2):69–76.
- [3] Wise C. Part 2 - Designing a meaningful structure. The Institution of Structural Engineers, editor. Essential Knowledge Text No2. IStructE Ltd; 2016.
- [4] Royal Ballet School: Bridge of Aspiration | WilkinsonEyre [Internet]. [cited 2021 Mar 12]. Available from: <https://www.wilkinsoneyre.com/projects/royal-ballet-school-bridge-of-aspiration>
- [5] BIG | Bjarke Ingels Group, KIS The Twist [Internet]. [cited 2021 Mar 12]. Available from: <https://big.dk/#projects-kis>
- [6] Lienhard J. Bending-active structures: form-finding strategies using elastic deformation in static and kinetic systems and the structural potentials therein. 2014.
- [7] Filz GH, Elmas S, Markou AA. Zero Gravity 2.0 Exhibition | Aalto University [Internet]. [cited 2021 Mar 12]. Available from: <https://www.aalto.fi/en/research-art/zero-gravity-20-exhibition>
- [8] Lienhard J, Knippers J. Bending-active textile hybrids. *Journal of the International Association for Shell and Spatial Structures*. 2015;56(1):37–48.
- [9] Knippers J, Jungjohann H, Scheible F, Oppe M. Bio-inspired Kinetic GFRP-façade for the Thematic Pavilion of the EXPO 2012 in Yeosu. *International Association for Shell and Spatial Structures (IASS)*. 2012;90(6):341–7.
- [10] Filz GH. Loop [Internet]. [cited 2021 Mar 16]. Available from: http://archiv.koge.at/?page_id=4202
- [11] Slabbinck ELM, Körner A, Knippers J. Torsion as a design driver in bending-active tensile structures. *International Association for Shell and Spatial Structures (IASS)*, 2017;1-10.
- [12] La Magna R, Schleicher S, Knippers J. Bending-Active Plates. *Advances in architectural geometry*, 2016; 170-87
- [13] Lienhard J, Alpermann H, Gengnagel C, Knippers J. Active bending, a review on structures where bending is used as a self-formation process. *International Journal of Space Structures*, 2013, 28.3-4: 187-196.
- [14] Finnish Forest Industries Federation, Schauman Wood Oy, Finnforest Oyj, Koskisen Oy VO. Handbook of finnish plywood. 2002.
- [15] Clove Hitch (Rope-End) | How to tie a Clove Hitch (Rope End) using Step-by-Step Animations | Animated Knots by Grog [Internet]. [cited 2021 Mar 12]. Available from: <https://www.animatedknots.com/clove-hitch-knot-rope-end>
- [16] McNeel R, Associates. Rhinoceros 3D, Version 6.0. Seattle, WA. 2010.

- [17] Dassault Systèmes. Abaqus Unified FEA - SIMULIA™ [Internet]. [cited 2021 Mar 16]. Available from: <https://www.3ds.com/products-services/simulia/products/abaqus/>
- [18] Clough RW, Penzien J. Dynamics of Structures. McGraw-Hill, New York; 1994.
- [19] Capturing Reality s.r.o. RealityCapture 2020 [Internet]. [cited 2021 Mar 16]. Available from: <https://www.capturingreality.com/>
- [20] Janiszewski M, Uotinen L, Rinne M, Baghbanan A. Digitisation of hard rock tunnel for remote fracture mapping and virtual training environment. ISRM International Symposium-EUROCK 2020. International Society for Rock Mechanics and Rock Engineering, 2020.
- [21] Ventsel E, Krauthammer T. Thin Plates and Shells. Thin Plates and Shells. 2001.
- [22] Kirchhoff G. Über das Gleichgewicht und die Bewegung einer elastischen Scheibe. J für die reine und Angew Math. 1850;40:51–88.
- [23] Von Karman TH. Encyklop die der Mathematischen. edition IV. Wissenschaften; 1910.